A THEORETICAL AND EXPERIMENTAL PERFORMANCE STUDY OF A ROOT-MUSIC ALGORITHM BASED ON A REAL-VALUED EIGENDECOMPOSITION

Marius Pesavento *Alex B. Gershman*

Department of ECE, McMaster University
Hamilton, Ontario, L8S 4K1 Canada
gershman@ieee.org

Martin Haardt

Siemens AG, ICN CA CTO 7
Hofmannstr. 51, Munich, Germany
Martin.Haardt@icn.siemens.de

ABSTRACT

A real-valued (unitary) formulation of the popular root-MUSIC Direction-Of-Arrival (DOA) estimation technique is considered. This unitary root-MUSIC algorithm is shown to reduce the computational complexity in the eigenanalysis stage of root-MUSIC, because it exploits the eigendecomposition of a real-valued covariance matrix. Theoretical, numerical, and experimental results are presented showing that, additionally, unitary root-MUSIC has improved threshold and asymptotic performances relative to conventional root-MUSIC. It can be then recommended that the former technique should always be preferred to the conventional root-MUSIC algorithm.

1. INTRODUCTION

The problem of reducing the computational complexity of eigenstructure methods via real-valued formulations has recently drawn a considerable attention in the literature [1]-[3].

In this paper, a unitary formulation of the root-MUSIC algorithm [4] is considered. First, the exact equivalence of this algorithm to the Forward-Backward (FB) root-MUSIC is shown. We stress, however, that unitary root-MUSIC has a simpler implementation than FB root-MUSIC because the former exploits the eigendecomposition of a real-valued matrix. Then, the asymptotic performance of the unitary root-MUSIC algorithm is studied. We prove that in situations with uncorrelated signal sources, the asymptotic performances of the unitary and conventional root-MUSIC algorithms are identical. However, in correlated and coherent source scenarios, the asymptotic performance of unitary root-MUSIC is shown to be better than that of conventional root-MUSIC. Simulation and experimental results are presented, demonstrating that unitary root-MUSIC outperforms conventional root-MUSIC in the threshold domain as well. As the unitary and conventional root-MUSIC algorithms are applicable to the same array configuration – Uniform Linear Arrays (ULA's), we conclude that *unitary root-MUSIC should be always preferred by the user to conventional root-MUSIC.*

Supported by the Natural Sciences and Engineering Research Council (NSERC) of Canada.

2. UNITARY ROOT-MUSIC

Let a ULA be composed of M sensors and let it receive q ($q < M$) narrowband signals impinging from the source directions $\theta_1, \ldots, \theta_q$. Assume that there are N snapshots $\mathbf{x}(1), \mathbf{x}(2), \ldots, \mathbf{x}(N)$ available. The $M \times 1$ array observation vector is modeled as [4]

$$\mathbf{x}(t) = \mathbf{A}\mathbf{s}(t) + \mathbf{n}(t)\,, \tag{1}$$

where $\mathbf{A} = [\mathbf{a}(\theta_1), \ldots, \mathbf{a}(\theta_q)]$ is the $M \times q$ matrix of the signal direction vectors, $\mathbf{a}(\theta) = [1, \exp\{j\,(2\pi/\lambda)\,d \sin\theta\}, \ldots, \exp\{j\,(2\pi/\lambda)\,d(M-1)\sin\theta\}]^T$ is the $M \times 1$ steering vector, $\mathbf{s}(t)$ is the $q \times 1$ vector of source waveforms, $\mathbf{n}(t)$ is the $M \times 1$ vector of white sensor noise, λ is the wavelength, d is the interelement spacing, and $(\cdot)^T$ stands for the transpose.

We introduce the $M \times M$ true and sample real-valued covariance matrices as [1]-[3]

$$\mathbf{C} = \mathbf{Q}^H \mathbf{R}_{\mathrm{FB}} \mathbf{Q}\,, \quad \hat{\mathbf{C}} = \mathbf{Q}^H \hat{\mathbf{R}}_{\mathrm{FB}} \mathbf{Q}\,, \tag{2}$$

where $\mathbf{R}_{\mathrm{FB}} = \frac{1}{2}(\mathbf{R} + \mathbf{J}\mathbf{R}^*\mathbf{J})$ and $\hat{\mathbf{R}}_{\mathrm{FB}} = \frac{1}{2}(\hat{\mathbf{R}} + \mathbf{J}\hat{\mathbf{R}}^*\mathbf{J})$ are the centro-Hermitian FB covariance matrix and its sample estimate, respectively. Here,

$$\mathbf{R} = \mathrm{E}\left\{\mathbf{x}(t)\mathbf{x}^H(t)\right\} = \mathbf{A}\mathbf{S}\mathbf{A}^H + \sigma^2 \mathbf{I} \tag{3}$$

is the conventional complex-valued covariance matrix, $\hat{\mathbf{R}} = \frac{1}{N}\sum_{k=1}^{N} \mathbf{x}(k)\mathbf{x}^H(k)$ is its sample estimate, $\mathbf{J}$ is the exchange matrix with ones on its antidiagonal and zeros elsewhere, $\mathbf{Q}$ is any unitary, column conjugate symmetric $M \times M$ matrix satisfying $\mathbf{J}\mathbf{Q}^* = \mathbf{Q}$ [2], $\mathbf{S} = \mathrm{E}\{\mathbf{s}(t)\mathbf{s}^H(t)\}$ is the $q \times q$ source waveform covariance matrix, $\mathbf{I}$ is the identity matrix, σ^2 is the noise variance, N is the number of snapshots, $(\cdot)^*$ denotes the complex conjugate, and $(\cdot)^H$ stands for the Hermitian transpose. The following sparse matrices [1]-[3]

$$\mathbf{Q} = \frac{1}{\sqrt{2}} \begin{bmatrix} \mathbf{I} & j\mathbf{I} \\ \mathbf{J} & -j\mathbf{J} \end{bmatrix}, \; \mathbf{Q} = \frac{1}{\sqrt{2}} \begin{bmatrix} \mathbf{I} & \mathbf{0} & j\mathbf{I} \\ \mathbf{0}^T & \sqrt{2} & \mathbf{0}^T \\ \mathbf{J} & \mathbf{0} & -j\mathbf{J} \end{bmatrix} \tag{4}$$

can be chosen for arrays with an even and odd number of sensors, respectively, where the vector $\mathbf{0} = (0, 0, \ldots, 0)^T$.

Let the eigendecompositions of the complex- and real-valued true covariance matrices be defined in a standard way [2]

$$\mathbf{R} = \mathbf{V}\mathbf{\Pi}\mathbf{V}^H = \mathbf{V}_S\mathbf{\Pi}_S\mathbf{V}_S^H + \sigma^2\mathbf{V}_N\mathbf{V}_N^H , \quad (5)$$

$$\mathbf{R}_{FB} = \mathbf{U}\mathbf{\Lambda}\mathbf{U}^H = \mathbf{U}_S\mathbf{\Lambda}_S\mathbf{U}_S^H + \sigma^2\mathbf{U}_N\mathbf{U}_N^H , \quad (6)$$

$$\mathbf{C} = \mathbf{E}\mathbf{\Gamma}\mathbf{E}^H = \mathbf{E}_S\mathbf{\Gamma}_S\mathbf{E}_S^H + \sigma^2\mathbf{E}_N\mathbf{E}_N^H , \quad (7)$$

where $\mathbf{V}_S = [\mathbf{v}_1, \ldots, \mathbf{v}_q]$, $\mathbf{V}_N = [\mathbf{v}_{q+1}, \ldots, \mathbf{v}_M]$, $\mathbf{\Pi}_S = \text{diag}\{\pi_1, \ldots, \pi_q\}$, $\mathbf{U}_S = [\mathbf{u}_1, \ldots, \mathbf{u}_q]$, $\mathbf{U}_N = [\mathbf{u}_{q+1}, \ldots, \mathbf{u}_M]$, $\mathbf{\Lambda}_S = \text{diag}\{\lambda_1, \ldots, \lambda_q\}$, $\mathbf{E}_S = [\mathbf{e}_1, \ldots, \mathbf{e}_q]$, $\mathbf{E}_N = [\mathbf{e}_{q+1}, \ldots, \mathbf{e}_M]$, $\mathbf{\Gamma}_S = \text{diag}\{\gamma_1, \ldots, \gamma_q\}$, and the subscripts S and N stand for signal- and noise-subspace, respectively. Similarly, the eigendecompositions of the sample covariance matrices can be defined as

$$\hat{\mathbf{R}} = \hat{\mathbf{V}}\hat{\mathbf{\Pi}}\hat{\mathbf{V}}^H = \hat{\mathbf{V}}_S\hat{\mathbf{\Pi}}_S\hat{\mathbf{V}}_S^H + \hat{\mathbf{V}}_N\hat{\mathbf{\Pi}}_N\hat{\mathbf{V}}_N^H , \quad (8)$$

$$\hat{\mathbf{R}}_{FB} = \hat{\mathbf{U}}\hat{\mathbf{\Lambda}}\hat{\mathbf{U}}^H = \hat{\mathbf{U}}_S\hat{\mathbf{\Lambda}}_S\hat{\mathbf{U}}_S^H + \hat{\mathbf{U}}_N\hat{\mathbf{\Lambda}}_N\hat{\mathbf{U}}_N^H , \quad (9)$$

$$\hat{\mathbf{C}} = \hat{\mathbf{E}}\hat{\mathbf{\Gamma}}\hat{\mathbf{E}}^H = \hat{\mathbf{E}}_S\hat{\mathbf{\Gamma}}_S\hat{\mathbf{E}}_S^H + \hat{\mathbf{E}}_N\hat{\mathbf{\Gamma}}_N\hat{\mathbf{E}}_N^H \quad (10)$$

Writing the characteristic equation for the matrix $\hat{\mathbf{R}}_{FB}$ as $\hat{\mathbf{R}}_{FB}\hat{\mathbf{u}} = \hat{\lambda}\hat{\mathbf{u}}$, we obtain that

$$\mathbf{Q}^H\hat{\mathbf{R}}_{FB}\hat{\mathbf{u}} = \mathbf{Q}^H\hat{\mathbf{R}}_{FB}\mathbf{Q}\mathbf{Q}^H\hat{\mathbf{u}} = \hat{\mathbf{C}}\mathbf{Q}^H\hat{\mathbf{u}} = \hat{\lambda}\mathbf{Q}^H\hat{\mathbf{u}} \quad (11)$$

Equation (11) can be identified as the characteristic one for the real-valued covariance matrix $\hat{\mathbf{C}}$ in (2). Hence, the eigenvectors and eigenvalues of the matrices $\hat{\mathbf{C}}$ and $\hat{\mathbf{R}}_{FB}$ are related as

$$\hat{\mathbf{E}} = \mathbf{Q}^H\hat{\mathbf{U}} , \quad \hat{\mathbf{\Gamma}} = \hat{\mathbf{\Lambda}} \quad (12)$$

The conventional root-MUSIC polynomial is given by

$$f_{\text{MUSIC}}(z) = \mathbf{a}^T(1/z)\hat{\mathbf{V}}_N\hat{\mathbf{V}}_N^H\mathbf{a}(z) , \quad (13)$$

where $\mathbf{a}(z) = [1, z, \ldots, z^{M-1}]^T$, $z = e^{j\omega}$, and $\omega = \frac{2\pi}{\lambda} d \sin\theta$. Similarly to (13), the FB root-MUSIC polynomial can be used:

$$f_{FB}(z) = \mathbf{a}^T(1/z)\hat{\mathbf{U}}_N\hat{\mathbf{U}}_N^H\mathbf{a}(z) \quad (14)$$

A simple manipulation with the use of (12) yields

$$\begin{aligned} f_{FB}(z) &= \mathbf{a}^T(1/z)\mathbf{Q}\mathbf{Q}^H\hat{\mathbf{U}}_N\hat{\mathbf{U}}_N^H\mathbf{Q}\mathbf{Q}^H\mathbf{a}(z) \\ &= \mathbf{a}^T(1/z)\mathbf{Q}\hat{\mathbf{E}}_N\hat{\mathbf{E}}_N^T\mathbf{Q}^H\mathbf{a}(z) \\ &= \tilde{\mathbf{a}}^T(1/z)\hat{\mathbf{E}}_N\hat{\mathbf{E}}_N^T\tilde{\mathbf{a}}(z) = f_U(z) , \end{aligned} \quad (15)$$

where the transformed manifold $\tilde{\mathbf{a}}(z) = \mathbf{Q}^H\mathbf{a}(z)$ should be exploited for the polynomial rooting in (15). The relationship between the standard and transformed manifolds follows from the expression for the real-valued true covariance matrix

$$\mathbf{C} = \mathbf{Q}^H\mathbf{A}\tilde{\mathbf{S}}\mathbf{A}^H\mathbf{Q} + \sigma^2\mathbf{Q}^H\mathbf{Q} = \tilde{\mathbf{A}}\tilde{\mathbf{S}}\tilde{\mathbf{A}}^H + \sigma^2\mathbf{I} , \quad (16)$$

where $\tilde{\mathbf{S}} = \frac{1}{2}\left(\mathbf{S} + \mathbf{D}\mathbf{S}^*\mathbf{D}^H\right)$, $\mathbf{D} = \text{diag}\{e^{-j\frac{2\pi}{\lambda}d(M-1)\sin\theta_1}, \ldots, e^{-j\frac{2\pi}{\lambda}d(M-1)\sin\theta_q}\}$, and $\tilde{\mathbf{A}} = \mathbf{Q}^H\mathbf{A}$.

Let us term the polynomial (15) as the unitary root-MUSIC polynomial since it exploits the eigendecomposition of the real-valued matrix $\hat{\mathbf{C}}$ instead of that of the complex-valued matrices $\hat{\mathbf{R}}$ and $\hat{\mathbf{R}}_{FB}$. From (15), it is clear that the FB and unitary root-MUSIC polynomials are identical. Hence, the performance of unitary root-MUSIC does not depend on a particular choice of the unitary matrix $\mathbf{Q}$, though (4) seems to be a very good choice because the matrix $\hat{\mathbf{C}}$ can be obtained from the matrix $\hat{\mathbf{R}}_{FB}$ with a very low computational cost. However, although both polynomials $f_{FB}(z)$ and $f_U(z)$ are proven to be identical, the computation of the coefficients of $f_U(z)$ is a simpler operation (if implemented via the real-valued eigendecomposition (10)), because the real-valued eigendecomposition has a reduced computational complexity than the complex one, approximately by a factor of four. Since the polynomial rooting is a much simpler operation than the eigendecomposition [5], we can conclude that the overall computational cost of unitary root-MUSIC is about four times lower than that of conventional root-MUSIC. We also stress that this conclusion cannot be extended to the unitary spectral MUSIC technique [1] because the main computational cost of spectral MUSIC is due to the exhaustive spectral search rather than the eigendecomposition.

3. PERFORMANCE ANALYSIS

Let us introduce the "eigenvector error" vector

$$\mathbf{g}_i = \hat{\mathbf{e}}_i - \mathbf{e}_i , \quad i = 1, \ldots, q \quad (17)$$

Then, the following lemma holds [6]:

Lemma 1: The signal-subspace eigenvector estimation errors (17) are asymptotically (for a large number of snapshots N) jointly Gaussian distributed with zero means and covariance matrices given by

$$\begin{aligned} \text{Cov}\{\mathbf{g}_i, \mathbf{g}_k\} = \frac{1}{N}\Bigg(&\sum_{\substack{l=1 \\ l\neq i}}^{q}\sum_{\substack{p=1 \\ p\neq k}}^{q} \frac{\Pi_{lpki}}{(\gamma_i - \gamma_l)(\gamma_k - \gamma_p)}\mathbf{e}_l\mathbf{e}_p^T \\ &+ \frac{\gamma_i\sigma^2}{2(\gamma_i - \sigma^2)^2}\mathbf{E}_N\mathbf{E}_N^T\delta_{ik}\Bigg) , \end{aligned} \quad (18)$$

where $\Pi_{lpki} = \frac{1}{2}(\gamma_i\gamma_p\delta_{ik}\delta_{lp} + \gamma_i\gamma_k\delta_{ip}\delta_{kl} + \mathbf{w}_l^T(\mathbf{e}_p\mathbf{e}_k^T + \mathbf{e}_k\mathbf{e}_p^T)\mathbf{w}_i)$, $\mathbf{w}_i = \text{Im}\left\{\mathbf{Q}^H\mathbf{R}\mathbf{Q}\right\}\mathbf{e}_i$, $1 \leq i, k \leq q$, and δ_{ik} denotes the Kronecker delta.

Following [4], we obtain that the DOA estimation Mean Square Error (MSE) of unitary root-MUSIC is given by

$$\text{E}\left\{(\hat{\theta}_i - \theta_i)^2\right\} = \left(\frac{\lambda}{2\pi d\cos\theta_i}\right)^2 \frac{\text{E}\left\{\hat{G}(\omega_i)\right\}}{4\left(\tilde{\mathbf{d}}^H(\omega_i)\mathbf{E}_N\mathbf{E}_N^T\tilde{\mathbf{d}}(\omega_i)\right)^2} , \quad (19)$$

where $\tilde{\mathbf{d}}(\omega) = d\tilde{\mathbf{a}}(\omega)/d\omega$,

$$\begin{aligned} \hat{G} = &\, 2\text{Re}\left\{\left(\tilde{\mathbf{d}}^H\left(\sum_{k=1}^{q}(\mathbf{e}_k\mathbf{g}_k^T + \mathbf{g}_k\mathbf{e}_k^T)\right)\tilde{\mathbf{a}}\right)^2\right\} \\ &+ 2\left|\tilde{\mathbf{d}}^H\left(\sum_{k=1}^{q}(\mathbf{e}_k\mathbf{g}_k^T + \mathbf{g}_k\mathbf{e}_k^T)\right)\tilde{\mathbf{a}}\right|^2 , \end{aligned} \quad (20)$$

and, for the sake of brevity, we denote $\hat{G} = \hat{G}(\omega_i)$, $\tilde{\mathbf{a}} = \tilde{\mathbf{a}}(\omega_i)$, and $\tilde{\mathbf{d}} = \tilde{\mathbf{d}}(\omega_i)$. Using Lemma 1, equation (19), and the readily verifiable properties $\mathbf{E}_N^T\tilde{\mathbf{a}} = \mathbf{0}$ and

$$\Pi_{iplk} = \Pi_{kpli} = \Pi_{ilpk} = \Pi_{klpi} , \quad (21)$$

we obtain that

$$\mathrm{E}\{\hat{G}\} = \frac{\sigma^2}{N}\sum_{k=1}^{q}\frac{\gamma_k}{(\gamma_k-\sigma^2)^2}\left(\mathrm{Re}\left\{(\mathbf{e}_k^T\tilde{\mathbf{a}})^2\,\tilde{\mathbf{d}}^H\mathbf{E}_{\mathrm{N}}\mathbf{E}_{\mathrm{N}}^T\tilde{\mathbf{d}}^*\right\} + |\mathbf{e}_k^T\tilde{\mathbf{a}}|^2\,\tilde{\mathbf{d}}^H\mathbf{E}_{\mathrm{N}}\mathbf{E}_{\mathrm{N}}^T\tilde{\mathbf{d}}\right) \quad (22)$$

In can be shown that $\tilde{\mathbf{d}}(\omega) = j\,\mathbf{Q}^H\boldsymbol{\Delta}\,\mathbf{Q}\,\tilde{\mathbf{a}}(\omega)$ where $\boldsymbol{\Delta} = \mathrm{diag}\{0,1,2,\ldots,M-1\}$. Also, it can be readily verified that $\mathbf{J}\mathbf{a}(\omega) = z^{M-1}\mathbf{a}^*(\omega)$, $\mathbf{J}\mathbf{Q}^* = \mathbf{Q}$, and $\mathbf{U}_{\mathrm{N}}^T = \mathbf{U}_{\mathrm{N}}^H\mathbf{J}$. Using all these properties and (12), we can prove that

$$(\mathbf{e}_k^T\tilde{\mathbf{a}})^2\,\tilde{\mathbf{d}}^H\mathbf{E}_{\mathrm{N}}\mathbf{E}_{\mathrm{N}}^T\tilde{\mathbf{d}}^* = -j|\mathbf{e}_k^T\tilde{\mathbf{a}}|^2\,(\tilde{\mathbf{d}}^H\mathbf{E}_{\mathrm{N}}\mathbf{E}_{\mathrm{N}}^T\mathbf{Q}^H\mathbf{J}\boldsymbol{\Delta}\mathbf{J}\mathbf{Q}\tilde{\mathbf{a}}) \quad (23)$$

Using the identities $\mathbf{E}_{\mathrm{N}}^T\tilde{\mathbf{a}} = \mathbf{0}$ and $\boldsymbol{\Delta} - (M-1)\mathbf{I} = -\mathbf{J}\boldsymbol{\Delta}\mathbf{J}$, it can be also shown that

$$-j\,\mathbf{E}_{\mathrm{N}}^T\mathbf{Q}^H\mathbf{J}\boldsymbol{\Delta}\mathbf{J}\mathbf{Q}\tilde{\mathbf{a}} = \mathbf{E}_{\mathrm{N}}^T\tilde{\mathbf{d}} \quad (24)$$

Inserting (24) into (23), we obtain

$$(\mathbf{e}_k^T\tilde{\mathbf{a}})^2\,\tilde{\mathbf{d}}^H\mathbf{E}_{\mathrm{N}}\mathbf{E}_{\mathrm{N}}^T\tilde{\mathbf{d}}^* = |\mathbf{e}_k^T\tilde{\mathbf{a}}|^2\,\tilde{\mathbf{d}}^H\mathbf{E}_{\mathrm{N}}\mathbf{E}_{\mathrm{N}}^T\tilde{\mathbf{d}} \quad (25)$$

Then, inserting (25) into (22) and using (12), we obtain from (19) our final expression for the DOA estimation MSE:

$$\mathrm{E}\left\{(\hat{\theta}_i-\theta_i)^2\right\} = \left(\frac{\lambda}{2\pi d\cos\theta_i}\right)^2\frac{\sigma^2\sum_{k=1}^{q}\frac{\lambda_k}{(\lambda_k-\sigma^2)^2}|\mathbf{u}_k^H\mathbf{a}|^2}{2N\,\mathbf{d}^H\mathbf{U}_{\mathrm{N}}\mathbf{U}_{\mathrm{N}}^H\mathbf{d}}, \quad (26)$$

where $\mathbf{d}(\omega) = d\mathbf{a}(\omega)/d\omega$ and the simplified notations $\mathbf{a} = \mathbf{a}(\omega_i)$ and $\mathbf{d} = \mathbf{d}(\omega_i)$ are used. Comparing (26) with the results derived by Rao and Hari (equations (26) and (28) in [4]), we see that the only difference between the MSE's of the conventional and unitary root-MUSIC algorithms is that our expression (26) for the unitary root-MUSIC MSE contains the eigenvectors and eigenvalues of the FB covariance matrix $\mathbf{R}_{\mathrm{FB}}$, whereas the aforementioned expressions in [4] contain the eigenvectors and eigenvalues of the conventional covariance matrix $\mathbf{R}$. Obviously, in uncorrelated source scenarios $\mathbf{R} = \mathbf{R}_{\mathrm{FB}}$, and, therefore, we conclude that the asymptotic performances of the unitary and conventional root-MUSIC algorithms are identical in this case. However, in situations with correlated or coherent sources, the asymptotic performance of unitary root-MUSIC is better than that of conventional root-MUSIC due to the FB averaging effect. This fact is clearly demonstrated in the next section by means of comparison of our analytical and simulation results.

4. SIMULATION RESULTS

We assumed a ULA of ten omnidirectional sensors with the half-wavelength interelement spacing, and two equally powered narrowband sources with the DOA's $\theta_1 = 10°$ and $\theta_2 = 15°$. A total of 1000 independent simulation runs have been performed with $N = 100$. In both our examples, the experimental DOA estimation Root-Mean-Square Errors (RMSE's) have been compared with the stochastic Cramér-Rao Bound (CRB) and with the results of our theoretical (asymptotic) analysis.

In the first and second examples, we assumed two uncorrelated and correlated sources (with the correlation coefficient equal to 0.99 and zero intersource phase in the first sensor), respectively. Figures 1 and 2 display the results for our examples.

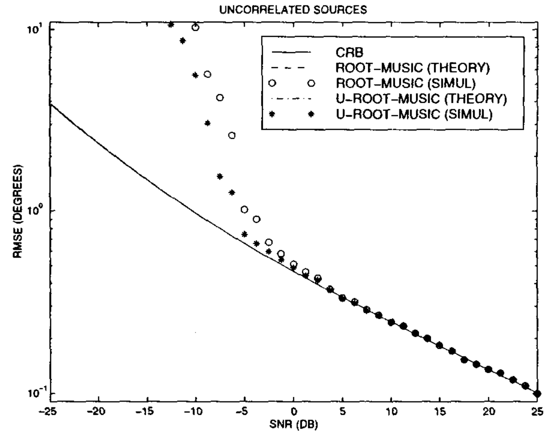

Figure 1: RMSE's vs. the SNR in the first example.

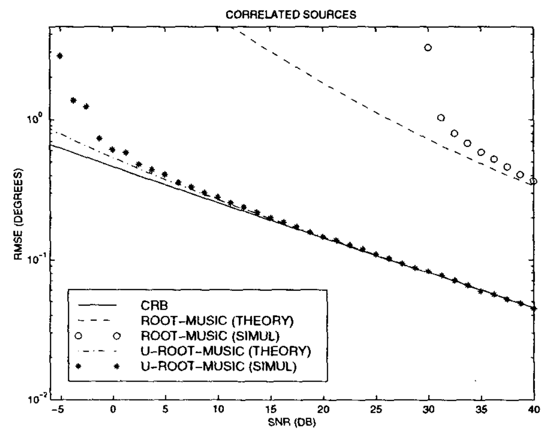

Figure 2: RMSE's vs. the SNR in the second example.

From these figures, we observe that there is an excellent correspondence of the theoretical curves and experimental points at a high SNR. As expected, for uncorrelated sources the asymptotic performances of both algorithms are identical. However, from the example with correlated sources, we see that the unitary root-MUSIC algorithm performs asymptotically better. Furthermore, in both examples unitary root-MUSIC has the lower SNR threshold than conventional root-MUSIC.

5. EXPERIMENTAL RESULTS

To compare the conventional and unitary root-MUSIC algorithms further, experimental sonar and ultrasonic ULA data have been used. The experiments were conducted by STN Atlas Elektronik, Bremen, in October 1983, in the Bornholm Deep, Baltic Sea. A horizontal ULA of 15 hy-

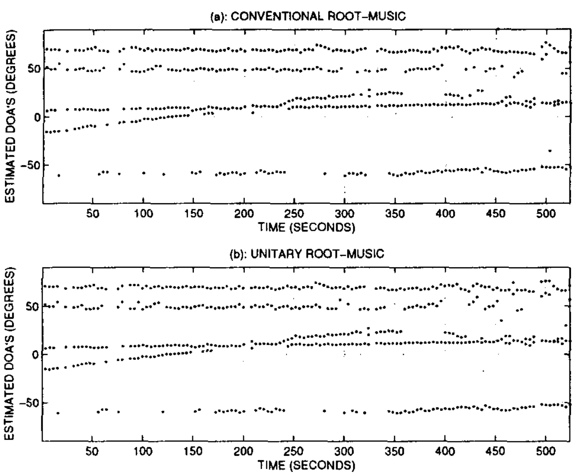

Figure 3: Results of the real sonar data processing.

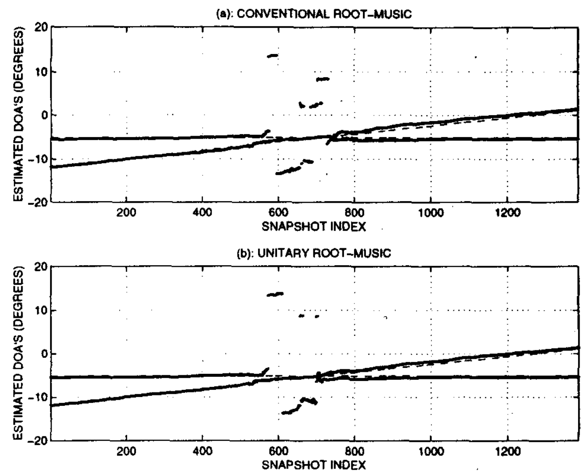

Figure 4: Results of the real ultrasonic data processing.

drophones was towed by a surface ship. The sea depth at the experimental site was about $60 - 65$ m. The towed receiving array had the interelement spacing $d = 2.56$ m, and the sampling frequency was $f_s = 1024$ Hz after lowpass filtering with the cutoff 256 Hz. The narrowband snapshots with the 4 Hz bandwidth have been formed from this broadband data after a DFT at the frequency bin $f = 240$ Hz. The sequence of covariance matrices has been estimated using nonoverlapping sliding windows with four seconds duration each.

Figs. 3 (a) and (b) show the results of real sonar data processing using conventional and unitary root-MUSIC, respectively. From this figure, we observe that both algorithms have nearly identical performance.

The employed ultrasonic data were recorded at University of Wyoming Source Tracking Array Testbed (UW STAT) [7]. These narrowband 6-element array data are available on the World Wide Web at `http://wwweng.uwyo.edu/electrical/array.html`. They have the carrier frequency 40 kHz and the signal bandwidth 200 Hz. The receiving ULA with the interelement spacing 2.1λ has been used.

A rectangular (maximal-overlap) sliding window with $N = 150$ snapshots has been employed to estimate the source trajectories. The results for conventional and unitary root-MUSIC are displayed in Fig. 4 (a) and (b), respectively. From these plots, we see that both algorithms have serious problems when the sources become closely spaced. However, from Fig. 4 we observe that unitary root-MUSIC has slightly better threshold performance than conventional root-MUSIC.

6. CONCLUSION

The real-valued formulation of root-MUSIC has been addressed. The unitary and FB root-MUSIC polynomials have been shown to be identical, but unitary root-MUSIC has a lower computational complexity than the conventional root-MUSIC technique. Closed-form expressions for the large sample MSE of unitary root-MUSIC have been derived and compared with the well-known results for conventional root-MUSIC. It has been shown that unitary root-MUSIC performs asymptotically similarly to or better than conventional root-MUSIC. Additionally, our simulations and real data examples have shown the better performance of unitary root-MUSIC in the threshold domain. Since the unitary and conventional root-MUSIC techniques are both applicable in the ULA case, we conclude that unitary root-MUSIC should be always preferred by the user to conventional root-MUSIC.

7. REFERENCES

[1] K.C. Huarng and C.C. Yeh, "A unitary transformation method for angle of arrival estimation," *IEEE Trans. ASSP*, **39**, pp. 975-977, 1991.

[2] D.A. Linebarger, R.D. DeGroat, and E.M. Dowling, "Efficient direction-finding methods employing forward-backward averaging," *IEEE Trans. SP*, **42**, pp. 2136-2145, 1994.

[3] M. Haardt and J.A. Nossek, "Unitary ESPRIT: How to obtain increased estimation accuracy with a reduced computational burden," *IEEE Trans. SP*, **43**, pp. 1232-1242, 1995.

[4] B.D. Rao and K.V.S. Hari, "Performance analysis of root-MUSIC," *IEEE Trans. ASSP*, **37**, pp. 1939-1949, 1989.

[5] M. Lang and B-C. Frenzel, "Polynomial root finding," *IEEE Signal Processing Letters*, **1**, pp. 141-143, 1994.

[6] G.M. Kautz and M. Zoltowski, "Performance analysis of MUSIC employing conjugate symmetric beamformers," *IEEE Trans. SP*, **43**, pp. 737-748, 1995.

[7] J.W. Pierre, E.D. Scott, and M.P. Hays, "A sensor array testbed for source tracking algorithms," *Proc. ICASSP'97*, Munich, pp. 3769-3772, 1997.